

# A facile method of fabricating mechanical durable anti-icing coatings based on CeO<sub>2</sub> microparticles

Pengren Wang<sup>1</sup>, Chaoyi Peng<sup>1,3</sup>, Binrui Wu<sup>1</sup>, Zhiqing Yuan<sup>2</sup>, Fubiao Yang<sup>1</sup> and Jingcheng Zeng<sup>1</sup>

<sup>1</sup>College of Aerospace Science and Engineering, National University of Defense Technology, Changsha, Hunan, 410073, People's Republic of China

<sup>2</sup>School of Packaging & Materials Engineering, Hunan University of Technology, Zhuzhou, Hunan, 412008, People's Republic of China

E-mail: 952639193@qq.com

**Abstract.** Compromising between hydrophobicity and mechanical durability may be a feasible approach to fabricating usable anti-icing coatings. This work improves the contact angle of current commercial anti-icing coatings applied to wind turbine blades dramatically and keeps relatively high mechanical durability. CeO<sub>2</sub> microparticles and diluent were mixed with fluorocarbon resin to fabricate high hydrophobic coatings on the glass fiber reinforced epoxy composite substrates. The proportion of CeO<sub>2</sub> microparticles and diluent influences the contact angles significantly. The optimum mass ratio of fluorocarbon resin to CeO<sub>2</sub> microparticles to diluent is 1:1.5:1, which leads to the highest contact angle close to 140°. The microscopy analysis shows that the CeO<sub>2</sub> microparticles form nano/microscale hierarchical structure on the surface of the coatings.

## 1. Introduction

Superhydrophobic surfaces with the water contact angle higher than 150° and the sliding angle less than 10° have attracted much attention in the past ten years [1-3]. There are many superhydrophobic surfaces in nature, and the best well-known example is the lotus leaf with the water contact angle of up to 160° [4, 5]. The SEM pictures of the lotus surface showed that the combination of micrometer/nanometer-scale roughness and epicuticular wax led to the superhydrophobic properties [6].

Superhydrophobic surfaces can be used in a variety of fields such as anti-icing, waterproof, self-cleaning, etc. Fabricating superhydrophobic surfaces includes two strategies: the one is constructing nano/microscale hierarchical structure on the intrinsic hydrophobic substrate, the other is modifying rough surface microstructures using low surface energy materials [7-9]. The common methods include template method [10], etching method [11], brush-coating [12], electrospinning technique [13], sol-gel method [14], layer-layer assembly [15-17], electrochemical deposition [2, 18, 19] etc.

However, most methods either have complicated processes or need expensive materials and experimental apparatus [20]. Thus, this is not conducive to large-scale production. Besides, for hydrophobic coatings, their mechanical durability is usually very poor and easily abraded by external forces [21]. Recent studies show that rare-earth metal oxide has not only good hydrophobicity but also

<sup>3</sup> Address for correspondence: Chaoyi Peng, College of Aerospace Science and Engineering, National University of Defense Technology, Changsha, Hunan, 410073, People's Republic of China, Email: 952639193@qq.com



durability properties [22]. CeO<sub>2</sub> is one kind of rare-earth metal oxide and has never been utilized to fabricate anti-icing coatings. Within, we report a simple method to fabricate a mechanical durable anti-icing coating by mixing CeO<sub>2</sub> microparticles and diluent with fluorocarbon resin. This method is easily controlled, and the raw materials are cheap [12, 20]. Furthermore, the coatings have good mechanical durability and can be cured at room temperature.

## 2. Experimental

### 2.1. Materials and method

Anti-icing coatings were made from the mixture of fluorocarbon resin (Obtained from Zhuzhou Times New Material Technology CO., LTD, China) with CeO<sub>2</sub> microparticles (obtained from Ganzhou Goring High-tech material Corporation Limited, China) and diluent. Diluent is the mixture of dimethylbenzene and butyl acetate (the mass ratio of dimethylbenzene to butyl acetate is 6:4). The curing agent is isocyanate (the ratio of resin to curing agent is 5:1). The diameter of CeO<sub>2</sub> microparticles is 10 μm.

Took 10 g fluorocarbon resin in the beaker, then diluent, CeO<sub>2</sub> microparticles and isocyanate were added to it in order. Finally, the mixture was homogeneously mixed by an electromagnetic stirrer. Took a certain amount of the coatings to brush on the composite material substrates and cured at room temperature.

We mainly studied the effects of the amount of CeO<sub>2</sub> microparticles and diluent on the hydrophobic properties of the coatings. Firstly, we studied the effects of diluent. The experimental formulations are shown in table 1.

**Table 1.** The experimental formulations of different amount of the diluent.

No.	Fluorocarbon resin (g)	Isocyanate (g)	Diluent (g)	CeO <sub>2</sub> microparticles (g)
A1	10	2	2.5	5
A2	10	2	5	5
A3	10	2	10	5
A4	10	2	20	5
A5	10	2	30	5
A6	10	2	40	5
A7	10	2	50	5

After finding the optimal amount of diluent based on the influence rules of which on the hydrophobic properties of the coatings, we changed the amount of CeO<sub>2</sub> microparticles to study the effects on the hydrophobicity of the coatings. The experimental formulations are shown in table 2.

**Table 2.** The experimental formulations of different amount of CeO<sub>2</sub>microparticles.

No.	Fluorocarbon resin (g)	Isocyanate (g)	Diluent (g)	CeO <sub>2</sub> microparticles (g)
B1	10	2	10	1
B2	10	2	10	3
B3	10	2	10	5
B4	10	2	10	8
B5	10	2	10	10
B6	10	2	10	15
B7	10	2	10	20

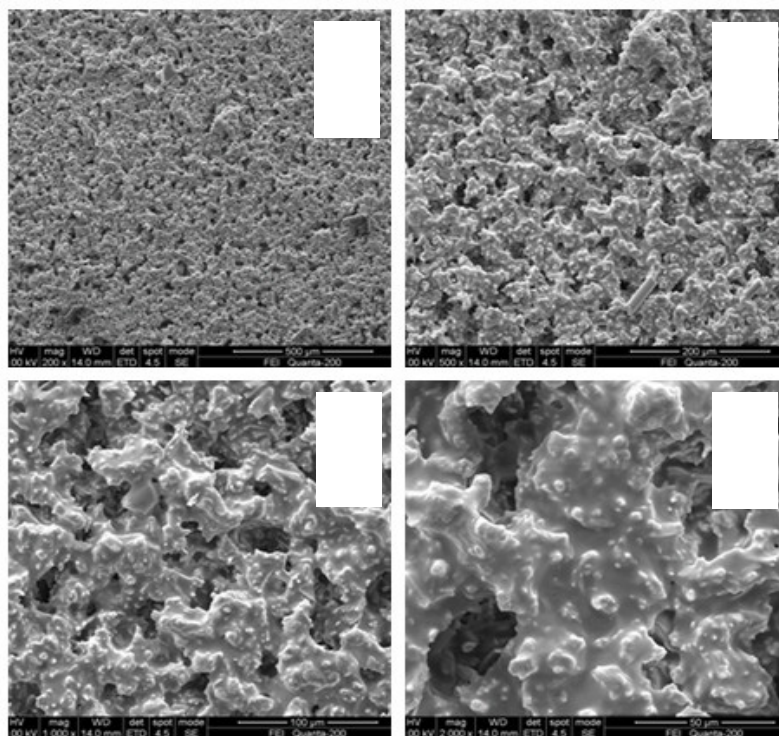


**Figure 1.** SEM pictures of anti-icing coatings whose mass ratio of fluorocarbon resin to  $\text{CeO}_2$  microparticles to diluent was 1:0.5:0.5. The scales of SEM pictures were 500  $\mu\text{m}$ , 200  $\mu\text{m}$ , 100  $\mu\text{m}$  and 50  $\mu\text{m}$  for a, b, c and d, respectively.

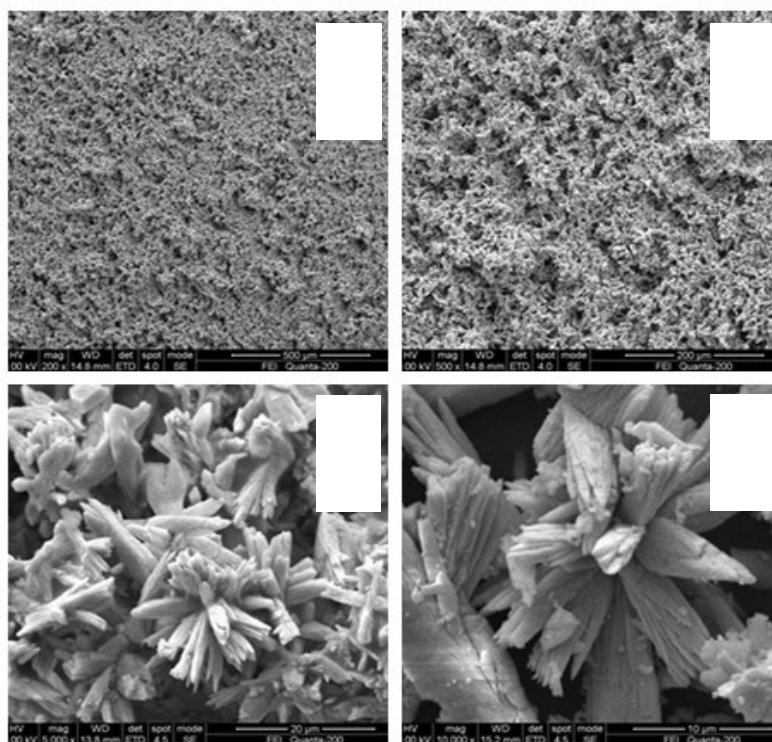


**Figure 2.** SEM pictures of anti-icing coatings whose mass ratio of fluorocarbon resin to  $\text{CeO}_2$  microparticles to diluent was 1:0.5:2. The scales of SEM pictures were 500  $\mu\text{m}$ , 200  $\mu\text{m}$ , 100  $\mu\text{m}$  and 50  $\mu\text{m}$  for a, b, c and d, respectively.

## 2.2. Characterization

The contact angle was measured by Standard Contact Angle Meter SL-200B (SHANGHAI SOLON INFORMATION TECHNOLOGY CO., LTD, China) in this work. A pipette was used to inject a water-drop on the surfaces of the coatings and the droplet formed a contact angle with the solid surface. The instrument was focalized to make the image of droplet showing on the screen clearly. After measuring the contact angle, the results were corrected by Elliptic Curve Method. Five different points of every sample were measured, and their averages were taken as the final results.

A scanning electron microscopy (SEM) of Quanta-200 (FEI Company, USA) was utilized to verify the nano/microscale hierarchical structures of the coatings. The samples were gold-sputtered before scanning. And then they were fixed on the sample plate to take photos under the vacuum condition.

## 3. Results and discussion

### 3.1. Surface morphology of coatings

Figures 1 and 2 display the results of SEM pictures of the obtained anti-icing coatings (the scales of SEM pictures are 500  $\mu\text{m}$ , 200  $\mu\text{m}$ , 100  $\mu\text{m}$  and 50  $\mu\text{m}$ , respectively). The mass ratio of fluorocarbon resin to  $\text{CeO}_2$  microparticles to diluents was 1:0.5:0.5. Figure 1 displays that the surface presented to be porous and the diameter of the micropore was about 10 $\mu\text{m}$ . The main substance of the surface was the cured rock-shaped resin and some bulges comprised of  $\text{CeO}_2$  microparticles were distributed on it. But the whole regularity was not good. The possible reason was the amount of resin was still large, and the  $\text{CeO}_2$  microparticles were resin-clad.

In figure 2, the amount of diluent increased. The mass ratio of fluorocarbon resin to  $\text{CeO}_2$  microparticles to diluent was 1:0.5:2. From the pictures, the surface still presented to be porous. An amount of chrysanthemum-shaped bulges were distributed on it. Nanoscale lamellar structures appeared on the tops of the chrysanthemum-shaped bulges. The combination of them constructed nano/microscale hierarchical structure.

From figures 1 and 2, the porous structure of the coatings surface and the bulges comprised of  $\text{CeO}_2$  microparticles became clearer and clearer with the increase of the amount of diluent. When diluent increased, the resin in per unit volume of the coatings became less, the  $\text{CeO}_2$  microparticles would not be resin-clad and could well subside on the surface to comprise nano/microscale hierarchical structure.

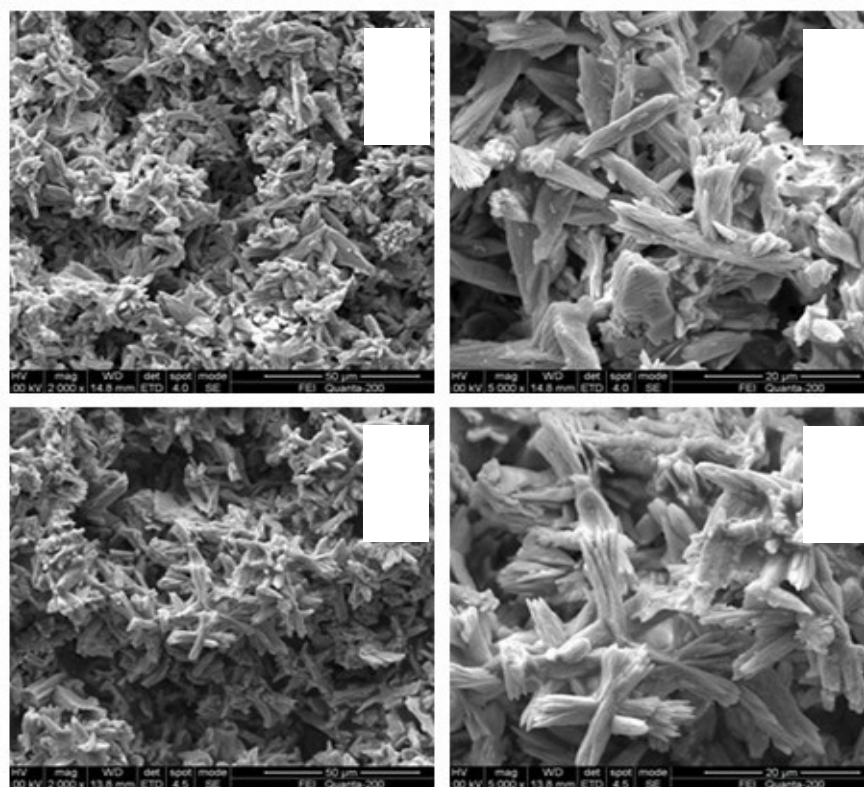
From figures 1 and 2, we also found that the  $\text{CeO}_2$  microparticles had different effects on the hydrophobicity of the coatings under the condition of two kinds of amounts of diluent. So we fixed the mass ratio of fluorocarbon resin to diluent to be 1:2, then changed the amount of  $\text{CeO}_2$  microparticles and observed the coatings microstructure. Under this condition, figure 3 shows the SEM pictures of anti-icing coatings whose mass ratio of fluorocarbon resin to  $\text{CeO}_2$  microparticles was 1:0.3 and 1:1, respectively.

Figure 3 shows that the microstructures of these two samples were very similar. They both presented to be rough and had flower-shaped bulges comprised of  $\text{CeO}_2$  microparticles. The results demonstrate that the change of the amount of  $\text{CeO}_2$  microparticles has little effects on the coatings microstructure under this condition.

### 3.2. Hydrophobic properties of coatings

The contact angles (CA) of the anti-icing coatings are shown in tables 3 and 4. The results in table 3 indicate the influence rules of diluent on the hydrophobicity of the coatings. It shows that when the mass ratio of fluorocarbon resin to diluent was bigger than 1:1, the CA was less than 70°. While the mass ratio was 1:1, the CA significantly increased to 137.88° which indicated the coatings already had good hydrophobic properties. It is because when the ratio was bigger than 1:1, the surface of the substrate was mainly covered by resin, so the  $\text{CeO}_2$  microparticles could not construct rough surface. But when the mass ratio was less than 1:1, the amount of resin decreased. So the sedimentary  $\text{CeO}_2$  microparticles which have hydrophobic properties formed the bulges and constructed the porous

chrysanthemum-shaped microstructure (shown in figure 2). As a result, the CA increased significantly. From table 3 we also found that when the mass ratio of fluorocarbon resin to diluent was less than 1:1, keeping adding diluent had little effects on the CA.



**Figure 3.** SEM pictures of anti-icing coatings. For a and b, the mass ratio of fluorocarbon resin to  $\text{CeO}_2$  microparticles to diluent was 1:0.3:2. For c and d, the mass ratio was 1:1:2. The scales of SEM pictures were 50  $\mu\text{m}$ , 20  $\mu\text{m}$ , 50  $\mu\text{m}$  and 20  $\mu\text{m}$  for a, b, c and d, respectively.

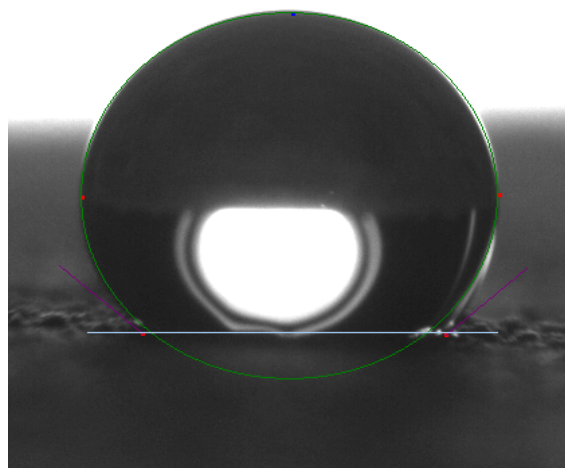


**Figure 4.** Water drop deposited on the anti-icing coatings surface: CA is 139.93.

Table 4 displays the influence rules of  $\text{CeO}_2$  microparticles on hydrophobic properties of the coatings under the condition of high diluents concentration. The highest CA in table 4 is close to  $140^\circ$  of which the mass ratio of fluorocarbon resin to  $\text{CeO}_2$  microparticles to diluent is 1:1.5:1 (shown in figure 4). The influence of  $\text{CeO}_2$  microparticles on the hydrophobic properties is not significant. In fact, when the amount of diluent is large, the  $\text{CeO}_2$  microparticles can be easily homogenized in the

coatings to construct nano/microscale hierarchical structure, so changing the amount of CeO<sub>2</sub> microparticles has little effects. Also, the CA became less with the decrease of CeO<sub>2</sub> microparticles. This is because when the particles decrease, there are fewer bulges on the coatings surface to construct nano/microscale hierarchical structure.

**Table 3.** Contact angles of anti-icing coatings (the mass ratio of fluorocarbon resin to CeO<sub>2</sub> microparticles is 1:0.5).

No.	Mass ratio of resin to diluent	CA (°)
A1	1 : 0.25	69.03
A2	1 : 0.5	65.40
A3	1 : 1	137.88
A4	1 : 2	136.45
A5	1 : 3	134.19
A6	1 : 4	138.62
A7	1 : 5	133.06

**Table 4.** Contact angles of anti-icing coatings (the mass ratio of fluorocarbon resin to diluent is 1:1).

No.	Mass ratio of resin to CeO <sub>2</sub> microparticles	CA (°)
B1	1 : 0.1	130.71
B2	1 : 0.3	131.93
B3	1 : 0.5	134.52
B4	1 : 0.7	128.11
B5	1 : 1	131.91
B6	1 : 1.5	139.93
B7	1 : 2	138.82

Recently, contact angles of most commercial anti-icing coatings for wind turbine blades are about 110° and these coatings are usually very weak to resist mechanical contact. In this work, we obtained coatings of which the highest water contact angle was close to 140°. Besides, these coatings also had good mechanical durability in theory.

#### 4. Conclusions

This work presented a facile method of fabricating mechanical durable anti-icing coatings based on CeO<sub>2</sub> microparticles that could be cured at room temperature. The SEM pictures indicate that the CeO<sub>2</sub> microparticles construct nano/microscale hierarchical structure on the surface of the coatings. The optimum mass ratio of fluorocarbon resin to CeO<sub>2</sub> microparticles to diluent is 1:1.5:1, which leads to the highest contact angle close to 140°, about 30° higher than commercial anti-icing coatings. Furthermore, these coatings can well resist mechanical contact theoretically. This method is simple and conducive to large-scale production. It will promote the hydrophobic surfaces to practical application in the future

#### References

- [1] Wang S and Jiang L 2007 Definition of superhydrophobic states *Advanced Materials* **19** 3423-4

- [2] Darmanin T, Givenchy E T D, Amigoni S, et al. 2013 Superhydrophobic surfaces by electrochemical processes *Advanced Materials* **25**1378-94
- [3] Erica Ueda and Pavel A Levkin 2013 Emerging applications of superhydrophilic-superhydrophobic Micropatterns *Advanced Materials* **25** 1234-47
- [4] Deng X, Mannen L, Butt H J, et al. 2012 Candle soot as a template for a transparent robust superamphiphobic coating *Science* **335** 67-70
- [5] Yao X, Song Y and Jiang L 2011 Applications of bio-inspired special wettable surfaces *Adv Mater* **23** 719-34
- [6] Barthlott W, Neinhuis C, Jetter R, et al. 1996 Waterlily, poppy, or sycamore: on the systematic position of *Nelumbo* *FLORA* **191** 169-74
- [7] Ma M and Hill R M 2006 Superhydrophobic surfaces *Current Opinion in Colloid & Interface Science* **11** 193-202
- [8] Feng L, Zhang Z, Mai Z, et al. 2004 A super-hydrophobic and super-oleophilic coating mesh film for the separation of oil and water *Angewandte Chemie (International ed. in English)* **43** 2012-4
- [9] Wu W, Wang X, Liu X, et al. 2009 Spray-coated fluorine-free superhydrophobic coatings with easy reparability and applicability *ACS Appl Mater Interfaces* **1** 1656-61
- [10] Feng L, Zhang Y, Xi J, et al. 2008 Petal effect: A superhydrophobic state with high adhesive force *Langmuir* **24** 4114-9
- [11] Öner D and McCarthy T J 2000 Ultrahydrophobic surfaces, effects of topography length scales on wettability *Langmuir* **16** 7777-82
- [12] Seyedmehdi S A, Zhang H and Zhu J 2013 Fabrication of superhydrophobic coatings based on nanoparticles and fluoropolyurethane *Journal of Applied Polymer Science* **128** 4136-40
- [13] Pisuchpen T, Chaim-ngoen N, Intasanta N, et al. 2011 Tuning hydrophobicity and water adhesion by electrospinning and silanization *Langmuir: the ACS Journal of Surfaces and Colloids* **27** 3654-61
- [14] Berendjchi A, Khajavi R, et al. 2011 Fabrication of superhydrophobic and antibacterial surface on cotton fabric by doped silica-based sols with nanoparticles of copper *Nanoscale Res Lett* **6** 594
- [15] Zhang M, Wang S, Wang C, et al. 2012 A facile method to fabricate superhydrophobic cotton fabrics *Applied Surface Science* **261** 561-6
- [16] Yang H, Dou X, Feng Y, et al. 2013 Self-assembled biomimetic superhydrophobic hierarchical arrays *J Colloid Interface Sci* **405** 51-57
- [17] Zhao Y, Xu Z, Wang X, et al. 2013 Superhydrophobic and UV-blocking cotton fabrics prepared by layer-by-layer assembly of organic UV absorber intercalated layered double hydroxides *Applied Surface Science* **286** 364-70
- [18] Peng S, Tian D, Miao X, et al. 2013 Designing robust alumina nanowires-on-nanopores structures: superhydrophobic surfaces with slippery or sticky water adhesion *Journal of Colloid and Interface Science* **409** 18-24
- [19] Valipour Motlagh N, Birjandi F C, Sargolzaei J, et al. 2013 Durable, superhydrophobic, superoleophobic and corrosion resistant coating on the stainless steel surface using a scalable method *Applied Surface Science* **283** 636-47
- [20] Tang Y, Yang J, Yin L, et al. 2014 Fabrication of superhydrophobic polyurethane/MoS<sub>2</sub> nanocomposite coatings with wear-resistance *Colloids and Surfaces A: Physicochemical and Engineering Aspects* **459** 261-6
- [21] Deng X, Mammen L, Zhao Y, et al. 2011 Transparent, Thermally Stable and Mechanically Robust Superhydrophobic Surfaces Made from Porous Silica Capsules *Advanced Materials* **23** 2962-5
- [22] Azimi G, Dhiman R, Kwon H M, et al. 2013 Hydrophobicity of rare-earth oxide ceramics *Nature Materials* **12** 315-20